ISSN: 2472-3703 DOI: 10.6911/WSRJ.202603_12(3).0009

Research on the Performance of SiC Particle Reinforced Aluminum Matrix Composite Brake Discs

Xiangling Wang [1, a, *], Xiaoling Shi [1], Zekai Qin [2]

[1]Department of Resources and Mechanical Engineering, Lyuliang University, Lvliang, Shanxi 033001, China

[2]School of Automotive Engineering, Tongji University, Shanghai 200092, China

[a]zbwxl05072402@163.com

[*] Corresponding author

Abstract

To meet the performance requirements of wear resistance, energy saving and consumption reduction during operation, as well as speed and noise reduction for rail transit brake discs, a SiC_p/A356 composite material with a SiC particle volume fraction of 20% was prepared by liquid stirring casting method using SiC particles as reinforcement and A356 aluminum alloy as matrix. Firstly, experiments were conducted on the thermal cycling characteristics, crack propagation, and fracture performance of the high-speed train brake disc made of this material. Secondly, a brake disc model was established using HYPERMESH software. Then, finite element simulation analysis of the temperature and stress fields under emergency braking conditions at 200km/h was conducted using ANSYS software to study the fracture failure mechanism. Compared with traditional steel brake discs, the results show that the maximum temperature during the braking process of SiC_p/A356 reinforced aluminum based composite brake discs is reduced by 29.6% compared to ordinary steel materials; The amplitude of stress changes is small, which can effectively reduce thermal damage to the surface of the brake disc; The fatigue life is increased by about 20% compared to ordinary steel materials, exhibiting excellent mechanical and fatigue properties.

Keywords

Liquid stirring casting method; Thermal cycling characteristics; Crack propagation; Finite element simulation analysis; Fracture failure mechanism; Fatigue life.

1. INTRODUCTION

In recent years, high-speed trains have developed rapidly and play a crucial role in China's rail transportation system, achieving a maximum operating speed of 350 km/h. Currently, most forged steel brake discs used in high-speed rail exhibit defects such as high mass, high energy consumption, and significant noise. Aluminum matrix composites, with their low density, high strength, low thermal expansion coefficient, corrosion resistance, and wear resistance [1], meet the developmental needs of lightweighting [2], energy efficiency, and noise reduction in rail transit. Among them, SiC particle-reinforced aluminum matrix composites, which have been extensively studied, offer advantages such as low cost and minimal damage to reinforcing elements during preparation, making them an ideal material for rail transit, aerospace, and national defense equipment.

Zhang Xin et al. [3] prepared SiC_p/2A50 aluminum matrix composites using the squeeze casting method, whose mechanical properties far exceeded those of the aluminum alloy matrix.

ISSN: 2472-3703 DOI: 10.6911/WSRJ.202603_12(3).0009

They concluded that the improvement in mechanical properties resulted from the combined effects of dislocation strengthening, interfacial strengthening, and aging strengthening, with a SiC particle volume fraction of around 20% yielding the best overall performance. Wu Zhaoling et al. [4] produced high-quality SiC_p/A356 aluminum matrix composites and pointed out that composite quality could be enhanced by controlling interfacial reactions, reducing gas content, refining grain size, and minimizing harmful inclusions. Cao Zilin et al. [5] noted that the liquid stirring casting method is cost-effective and highly efficient, requiring only traditional melting and casting processes, making it suitable for large-scale production. However, inert gas protection is necessary to minimize oxidation when adding reinforcements to molten liquid. Liu Chunxuan et al. [6] indicated that the three process parameters—stirring speed, stirring time, and stirring temperature—significantly influence the uniformity of reinforcement particles in the matrix, with their impact decreasing in order. When the reinforcement particle content exceeds 20%, particle agglomeration tends to occur. Cai Xiang et al. [7] observed that in aluminum matrix composites with varying SiC particle volume fractions prepared via powder extrusion molding, when the SiC particle volume fraction reached 30% and 40%, the increasing SiC content led to particle fracture during extrusion, resulting in reduced plasticity, as well as decreased strength and thermal expansion coefficient.

The efficiency and safety of high-speed train operation have received widespread attention in recent years. As the core component of the braking system, the brake disc is subjected to high temperature and high wear under high-speed operation and frequent braking load conditions. Yang Yue et al. [8] conducted elastic-plastic finite element simulation analysis on particle reinforced aluminum based composite brake discs and found that the mechanism of interface cracking is the effect of thermal tensile stress generated when the brake disc temperature cools from high temperature to room temperature after braking. Zhang Junqing et al. [9] combined the crack formation life obtained from the thermal fatigue test of SiC_p/A356 aluminum based composite brake discs with finite element simulation to establish a thermal fatigue strain life curve, providing a basis for subsequent thermal fatigue performance evaluation and life estimation.

In summary, a SiC_p/A356 composite material with a SiC particle volume fraction of 20% was prepared using the stirring casting method. The mechanical properties, crack propagation, and fracture mechanism of the high-speed train brake disc were tested by monotonic tensile tests at room temperature and high temperature, fracture toughness tests, fatigue crack propagation threshold and crack propagation rate tests at room temperature and low cycle. The fatigue life was analyzed using finite element simulation software and compared with that of traditional steel brake discs, aiming to provide theoretical basis for optimizing the performance of rail transit brake discs.

2. EXPERIMENTAL MATERIALS AND METHODS

2.1. Material Selection and Preparation

The matrix material is cast aluminum alloy A356, and the reinforcement material is SiC particles with an average particle size of 15 μm. The chemical composition is shown in Table 1.

The proportion of Si and Mg is crucial in aluminum alloy A356. Adding Si helps to improve the wear resistance and flowability of the material, and can suppress the formation of brittle phase Al_4C_3. Adding Mg can refine the microstructure and improve the wettability between SiC particles and aluminum liquid [10].

ISSN: 2472-3703 DOI: 10.6911/WSRJ.202603_12(3).0009

Table 1. Chemical Composition of Matrix and Reinforcement

Completion	Component	Content (mass fraction, %)
Aluminum alloy A356	Si	7.5
	Mg	0.45
	Fe	≤ 0.2
	Ti	≤ 0.2
	Cu	≤ 0.1
	Mn	≤ 0.1
	Zn	≤ 0.1
	Al	Bal.
SiC particles	SiC	97.8
	C	0.35
	Si	0.74
	SiO_2	0.71
	Fe_2O_3	0.40

SiC_p/A356 composite materials were prepared by liquid stirring casting method. Firstly, heat the A356 aluminum alloy ingot to a liquid state and control the temperature at 730 ℃. Secondly, add the SiC particles pre treated at 600 ° C for three hours to the A356 aluminum alloy melt at a volume fraction of 20%, and stir thoroughly in a vacuum environment until the lower limit temperature of 610 ℃ is reached. Further increase the temperature to 730 ℃ for pouring to obtain SiC_p/A356 composite material. Suitable process parameters such as stirring speed, stirring time, and stirring temperature are selected throughout the entire stirring casting process, and inert gas Ar protection is required throughout the stirring process to prevent oxidation of the melt.

The microstructure of SiC_p/A356 composite material was observed using scanning electron microscopy, as shown in Figure 1. There was no obvious agglomeration of SiC particles, and the particle distribution was relatively uniform, with a tight bond with the matrix [8, 11].

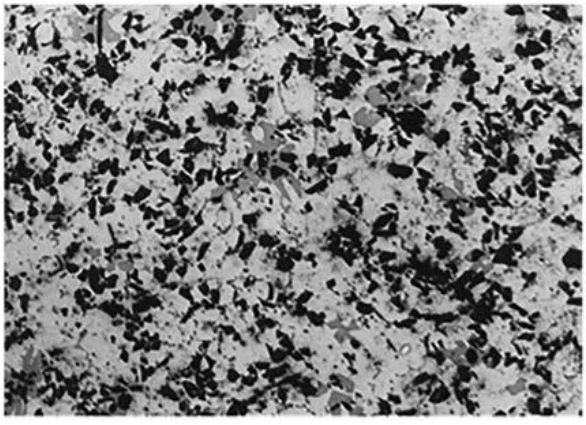

Figure 1. Microstructure of SiC_p/A356 Composite Material

2.2. Monotonic Tensile Test

The experiment uses a round bar specimen with a total length of 170 millimeters, an equivalent cross-sectional length of 86 millimeters in the middle, and a diameter of 15 millimeters. The transition section is circular R15, and the diameter of the two clamping sections is 15mm. The monotonic tensile test is conducted at room temperature and high temperature, with test temperatures of 25 ° C, 200 ° C, 300 ° C, and 400 ° C. The test is conducted using a room temperature extensometer and a high temperature extensometer, respectively,

ISSN: 2472-3703 DOI: 10.6911/WSRJ.202603_12(3).0009

and inert gas argon protection is required for the high temperature test at 400 ° C. The strain amplitude control method with an average strain of zero is adopted, and a triangular wave is used to maintain a constant strain rate of 0.004/s in one load cycle. The experimental values at each temperature are the average of 5 effective values, as shown in Figure 2 as the curve.

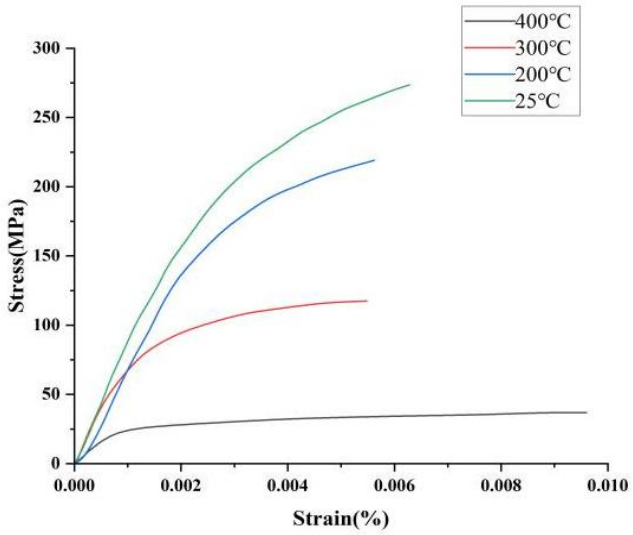

Figure 2. Curve of Monotonic Tensile Test

According to the test results in Figure 2, the thermoelastic - plastic constitutive relationship of the material was constructed using the R - O constitutive relationship model, as shown in Equation (1):

$$\varepsilon = \frac{\sigma}{E} + \left(\frac{\sigma}{K}\right)^{\frac{1}{n}},\ \sigma = K\varepsilon_p^n,\ K = \frac{\sigma_f}{\varepsilon_f^n} \tag{1}$$

In Equation (1), σ is the stress, E is the elastic modulus, n and K are the strengthening exponent and strengthening coefficient respectively, ε_p is the plastic strain, σ_f is the true fracture strength, and ε_f is the true fracture ductility.

The parameters obtained by fitting the curve shown in Figure 2 using the least squares method are shown in Table 2. The elastic modulus, yield strength, and tensile strength values of the material all show a decreasing trend with increasing temperature. When the temperature reaches 400 ℃, the elastic modulus decreases to 0.64 times that at room temperature.

Table 2. Analysis Results of Monotonic Tensile Properties Parameters of SiC_p/A356 Composite Material

Temperature/℃	E/GPa	σ_S/MPa	σ_b/MPa	n	K	r
25	108	263	312	0.1874	987.2	0.995
200	92.3	212	225	0.1751	654.1	0.979
300	81.4	134	118	0.1301	248	0.989
400	68.6	58.1	37.7	0.0984	40.4	0.981

2.3. Fracture Toughness Test

Finite element analysis shows that after multiple braking cycles, the residual stress inside the brake disc changes, indicating that the brake disc will eventually fracture under cyclic stress. During the operation and braking process of the actual brake disc, the consequences of fracture are very serious. Therefore, three three-point bending specimens were used to conduct low cycle fatigue fracture toughness tests on the composite brake disc at room temperature. B. W and a represent the thickness, width, and crack length of the sample, respectively. The size of the sample should ensure a small-scale yield state, that is: B, a, W-a $\geq 2.5(K_{IC}/\sigma_s)^2$. The

ISSN: 2472-3703 DOI: 10.6911/WSRJ.202603_12(3).0009

average value of the fracture section B/4, B/2, and 3B/4 was taken in this experiment. During the experiment, the specimen is first slotted and then fatigue cracks are prefabricated. When the load reaches the critical value of the stress intensity factor corresponding to unstable propagation, the fracture toughness K_{IC} is obtained. The test results are shown in Table 3.

Table 3. Fracture Toughness Test Results of SiCp/A356 Composite Material

Sample No.	1#	2#	3#
Test Value (MPa · $\sqrt{m}$)	14.8	13.9	15.1

For safety reasons, the minimum value of sample 2#, that is, K_{IC} = 13.9MPa•m$^{1/2}$, was taken as the fracture toughness of the SiC_p/A356 composite material.

2.4. Crack Propagation Threshold and Crack Propagation Rate Test

In actual train operation, the brake discs undergo multiple thermal cycles, exacerbating the thermal fatigue problem of the brake discs. This experiment used three compact tensile specimens to test the low cycle fatigue crack propagation rate of the composite brake disc at room temperature. The MTS810 testing machine was used for loading, with a cycle number N of 2500, a specimen length of 80cm, and a thickness of 9cm. The curve was drawn based on the test data as shown in Figure 3. When the number of cycles N is less than 1000, it is the stage of crack initiation. When 1000<N<2200, it is in the stage of stable crack propagation. After N>2200, it enters the stage of rapid crack propagation. The overall relationship between the crack length and the number of cycles of the three samples is roughly similar, but due to process differences in the preparation and processing of the samples, the crack lengths of the three samples are different in the test results, with sample 1# having the fastest crack propagation.

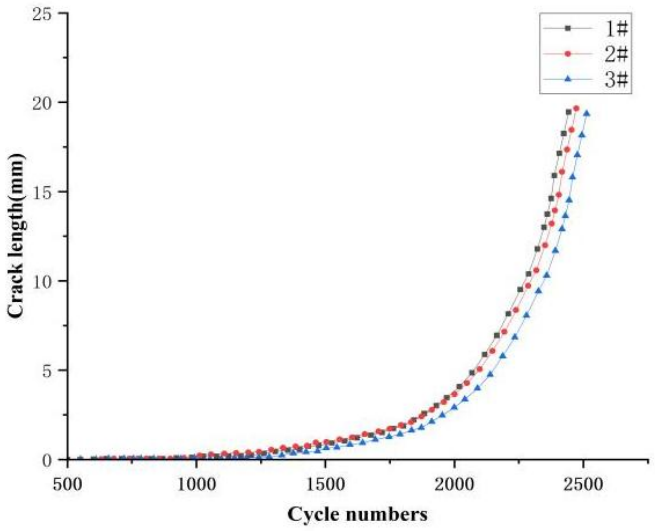

Figure 3. Test Data of Low Cycle Fatigue Crack Propagation Rate

At the same time, the fatigue crack propagation threshold ΔK_{th} of the SiC_p - reinforced aluminum matrix composite measured by the test is 2.64MPa·m$^{1/2}$, The fracture toughness is 13.9MPa·m$^{1/2}$, therefore 2.64-13.9cis used as the effective range for linearly fitting the crack propagation rate ($\frac{da}{dN}$-ΔK). The fatigue crack propagation rate curve is usually expressed by the Paris formula $da/dN = C(\Delta K)^m$ [11], Figure 4 shows the $da/dN - \Delta K$ curve in stable crack propagation stage of sample 1#.

ISSN: 2472-3703 DOI: 10.6911/WSRJ.202603_12(3).0009

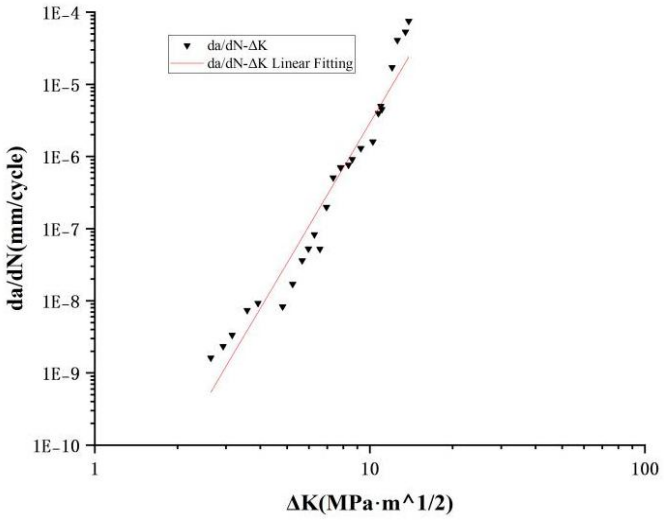

Figure 4. Curve of $da/dN - \Delta K$ Crack Propagation Rate

By taking the logarithm of both sides of $da/dN = C(\Delta K)^m$ and comparing it with the linear regression result y=A+BX, it can be concluded that:

$$m = B,\ A = lg\ C \tag{2}$$

The above fitting results are A = -10.932, B = 5.6843. After calculation, it is found that C=1.1684×10-11; m=5.6843, The regression result of the fatigue crack propagation rate of the material is: $da/dN = 1.1684 \times 10^{-11}(\Delta K)^{5.6843}$.

3. RESULTS AND DISCUSSION

Taking SiC_p aluminum based composite brake discs as the research object, due to the fact that the brake disc is a rotating body, its geometric model, stress, and temperature field distribution are all symmetrical to the rotation axis. Heat input and dissipation remain constant and axisymmetric during each rotation of the brake disc. Therefore, hexahedral mesh partitioning was adopted to simulate the temperature field [12] and stress field [13] distribution under emergency braking conditions at 200km/h, and to analyze the thermodynamic performance of composite brake discs. The braking parameters are shown in Table 4. When the brake shoe slides on the brake disc, the heat flux input of the disc surface friction is equal to the work done by the sliding friction force of the brake shoe on the brake disc friction surface per unit time, that is:

$$W = \eta F v(r,t) = \eta \cdot \mu p(r) \cdot v(r,t) \tag{3}$$

Heat flux density $q = W/S$, where S is the effective area of the friction surface, which is $0.154m^2$. In the formula, η is the energy distribution ratio, taken as 0.8. F is the sliding friction force, $F = \mu p(r)$, μ is the coefficient of friction, $p(r)$ is the pressure for brake disc brake pads, calculated as $F = 0.443 \times 17.3 \times 10^3 = 7664N$. $v(r,t)$ is the relative linear velocities at any point on the friction ring between the brake pad and the brake disc, $v(r,t) = (v_0 - at) \cdot 2r/D$, v_0, a, r, D are respectively the initial braking velocity, braking deceleration, friction radius, and wheel diameter. Assuming the braking process adopts uniform deceleration, then $a = 200/(3.6 \times 40.6) = 1.368m/s^2$. Through calculation, the heat flux density is: w=646670.3-15910.9t.

ISSN: 2472-3703 DOI: 10.6911/WSRJ.202603_12(3).0009

Table 4. Braking Parameters

Braking Parameter	initial velocity (km/h)	Brake Shoe Pressure (KN)	Friction Coefficient	Brake Distance (m)	Brake Deceleration (m/s^2)	Brake Time (s)
Emergency Braking	200	17.5	0.443	1100	1.368	40.6 s

After thermal analysis, the temperature fields of the ordinary steel material and the composite brake disc under one emergency braking condition are shown in Figure 5, and the thermal stress change curve obtained by applying the temperature field result to the structural analysis is shown in Figure 6.

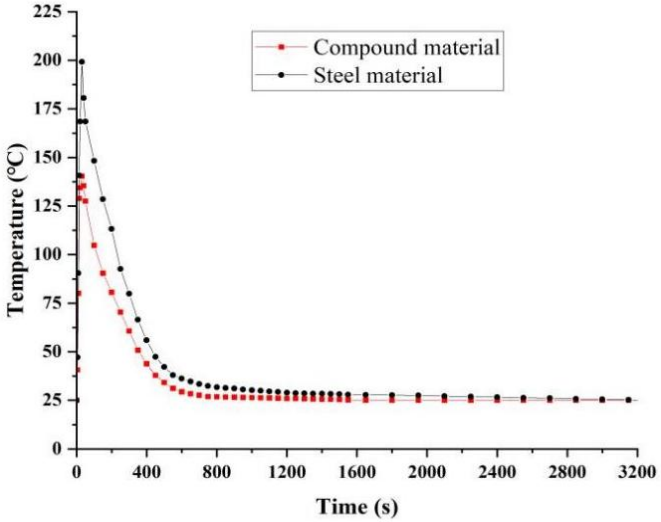

Figure 5. Curve of Temperature Change Under Emergency Braking Conditions

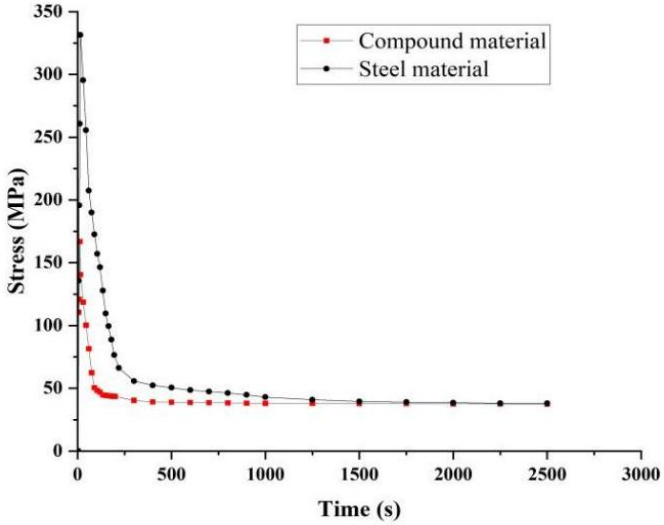

Figure 6. Curve of Thermal Stress Variation Ander Emergency Braking Conditions

It can be seen from Figures 5 - 6 that: (1) After the start of emergency braking, due to the strong heat flux input generated by friction, the temperature of the disc surface rises rapidly and reaches the peak point, and then the temperature gradually decreases because the disc surface transfers heat to the inside through heat conduction due to convective heat transfer. (2)

ISSN: 2472-3703 DOI: 10.6911/WSRJ.202603_12(3).0009

The temperature field distributions of the two materials are relatively similar. The maximum temperature during braking occurs at about 28s of braking, but the maximum temperature of the composite brake disc is significantly lower than that of the steel material, with a temperature reduction of 29.6%. Moreover, the temperature of the composite material drops to room temperature at about 1650s of braking, while the steel material drops to room temperature at about 3300s. (3) The stress of both materials reaches the maximum at about 12s of braking, the maximum stress of the composite material is lower than that of the steel material. After emergency braking, the thermal residual stress of the brake disc is not significantly different, both being 38 MPa. This means that the stress change amplitude of the composite brake disc is small, which can effectively reduce thermal damage to the surface of the brake disc.

Here, the conventional braking condition after emergency braking was used to analyze the crack propagation life. The stress field amplitude was taken as the driving force for the crack propagation of the brake disc, and the initial crack was 5mm. The Forman formula [14] was used to calculate the total crack propagation life of the aluminum matrix composite and the traditional steel material respectively, as shown in Figure 7. During the calculation, the influence of stress, threshold value and fracture toughness on the crack propagation life should be considered.

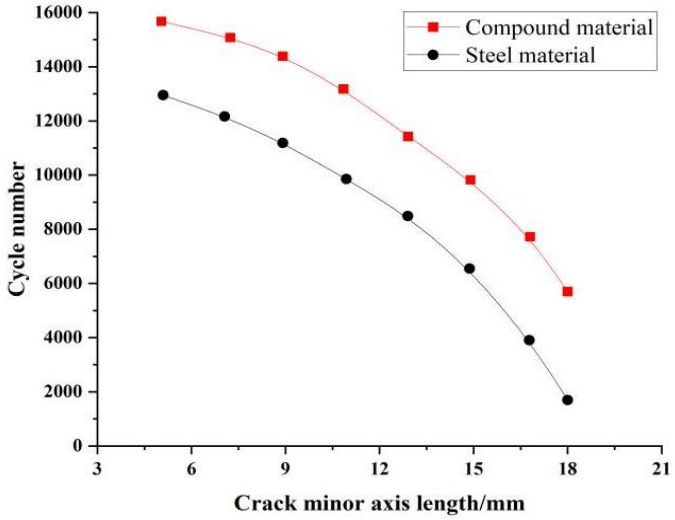

Figure 7. Curve of Crack Propagation Life

It can be seen from Figure 7 that: (1) The smaller the crack length a, the slower the crack propagation rate and the longer the lifespan. (2) When the crack length $5mm < a < 15mm$, the crack propagation rate is relatively stable, and the lifespan during this stage accounts for approximately 71.1% of the total propagation lifespan. when 15mm < a ≤ 18mm, the crack propagation rate accelerated, and the lifespan during this stage accounted for about 18.2% of the total propagation lifespan. when a > 18mm, the crack propagation rate was very fast, and the lifespan during this stage accounted for about 10.7% of the total propagation lifespan. To a large extent, severe braking accidents occurred, so it was necessary to replace the brake disc in a timely manner to avoid accidents; (3) The fatigue life of SiC_p reinforced aluminum based composite brake discs is significantly improved compared to traditional steel brake discs, with an increase of about 20% compared to ordinary steel materials, exhibiting excellent mechanical and fatigue properties.

4. CONCLUSIONS

The following conclusions can be drawn from experimental and simulation results:

ISSN: 2472-3703 DOI: 10.6911/WSRJ.202603_12(3).0009

(1) The low cycle fatigue test at room temperature of SiC_p reinforced aluminum based composite brake discs showed that the threshold value for fatigue crack propagation ΔK_{th} was 2.64 MPa•$m^{1/2}$, and the fracture toughness was 13.9 MPa•$m^{1/2}$. The effective range from 2.64 MPa•$m^{1/2}$ to 13.9 MPa•$m^{1/2}$ was the stable crack propagation stage.

(2) Under emergency braking conditions, the maximum temperature of SiC_p reinforced aluminum based composite brake discs is significantly lower than that of steel materials, with a temperature reduction of 29.6%. The stress variation amplitude of SiC_p reinforced aluminum based composite brake discs is small, which can effectively reduce thermal damage to the surface of the brake disc.

(3) Compared with the traditional steel material brake disc, the fatigue life of the SiC_p-reinforced aluminum matrix composite brake disc is significantly improved, with an increase of about 20% compared to ordinary steel materials, showing excellent mechanical and fatigue properties.

ACKNOWLEDGEMENTS

This work was supported by Key R&D Projects in Lvliang City (2023GXYF11, 2023GXYF12), Basic Research Program of Shanxi Province (202203021222316), Ministry of Education Industry-University-Research Cooperative Education Program Project (220501867165955).

REFERENCES

[1] Lu Jianning, Wang Juan, Zheng Kaihong, Long Jun. Microstructure and Electrical Conductivity of High Volume Fraction SiCp/A356 Composites [J]. Materials Review, 2018, 32(05): 257 - 260.

[2] Ma Zhiying, Li Rong, Cai Ziyi. Research on Multi - Objective Selection Method for High - Speed Train Wheel Sets [J]. Mechanical Design and Manufacture, 2020, 12(12): 277 - 281.

[3] Zhang Xin, Yao Shasha, Wang Changshun, et al. Research on the Microstructure and Mechanical Properties of SiCp/2A50 Aluminum Matrix Composites by Squeeze Casting [J]. New Technology and New Process, 2010, 06: 107 - 110.

[4] Wu Zhaoling, Han Jianmin, Li Weijing, Wang Jinhua. Preparation Quality Inspection and Control of SiCp/A356 Composite Materials [J]. Journal of Beijing Jiaotong University, 2006, 30(01): 100 - 106.

[5] Cao Zilin, Zhang Linhui, Zhong Binnian, et al. Preparation and Research Status of Aluminum Matrix Composites [J]. Metal Functional Materials, 2023, 30(02): 30 - 39.

[6] Liu Chunxuan, Luo Ren, Xie Yi. Research and Progress on Particle - Reinforced Aluminum Matrix Composites for Rail Transit Brake Discs [J]. Modern Urban Rail Transit, 2022, 07: 11 - 16.

[7] Cai Xiang, Zhang Hui, Chen Shuang, et al. Microstructure and Properties of SiCp/Al Composites Prepared by Powder Extrusion Forming [J]. Journal of Mechanical Engineering Materials, 2017, 41(07): 43 - 48 + 53.

[8] Yang Yue. Research on Thermal Fatigue Evaluation Method of SiCp/A356 Composite Brake Disc for High - Speed Trains [D]. Beijing: Beijing Jiaotong University, 2009: 12 - 13.

[9] Zhang Junqing, Zhou Suxia, Yang Yue. Research on Thermal Fatigue Properties of SiCp/A356 Particle Reinforced Aluminum Matrix Composite for High - Speed Train Brake Discs [J]. Engineering Mechanics, 2011, 28(08): 252 - 256.

[10] Chen Yixin, Wang Richu, Wang Xiaofeng, et al. The Effect of Mg on the Microstructure and Properties of SiCp/Al Composite Materials by Vacuum Pressure Infiltration [J]. Chinese Journal of Nonferrous Metals, 2016, 26(06): 122.

ISSN: 2472-3703 DOI: 10.6911/WSRJ.202603_12(3).0009

[11] Wang Xiangling, Shi Xiaoling. Mechanical Properties of SiC Whisker - Reinforced Aluminum Matrix Composite Wheel [J]. Science of Advanced Materials, 2021, 13(11): 2243 - 2249.

[12] Wu Bo, Sun Lei. Research on Transient Temperature Field of Brake Disc Based on Fluid - Solid Coupling Heat Transfer [J]. Mechanical Design and Manufacture, 2020, 6(06): 117 - 120.

[13] Huang Jian, Kong Lingyang, Li Weimin. Analysis of Temperature and Stress Fields of Disc Brakes [J]. Mechanical Design and Manufacture, 2015, (02): 143 - 145.

[14] Shi Xiaoling. Research on Thermal Fatigue Life Evaluation of Forged Steel Brake Discs for High - Speed Trains [D]. Beijing: Beijing Jiaotong University, 2017: 112 - 115.